

# FOUNDRY PRACTICE 259

FEBRUARY 2014



THE AUTHORITATIVE MAGAZINE FOR FOUNDRY ENGINEERS



ROTARY DEGASSING

COATING PREPARATION PLANT

IRON TURBULENCE ANALYSIS

CERAMIC FOAM FILTERS

# FOUNDRY PRACTICE 259

THE AUTHORITATIVE MAGAZINE FOR FOUNDRY ENGINEERS

FEBRUARY 2014

## 02 ROTARY DEGASSING



Degassing efficiency of different rotor design over rotor life

Author/s: Ronny Simon and Roger Kendrick, Foseco Europe



Hydrogen removal and control are a vital part of the metal treatment process in Aluminium casting production. Many years ago the options were only chemical addition in tablet form or inert gas bubbled through a lance. Degassing times were long and often the bottleneck in production but this situation changed with the introduction of rotary degassing. The use of highly efficient pumping rotors has now given the foundry the option of removing hydrogen in a short time. Rotary degassing is now the industry standard but a greater understanding is required for full process control. This study looks at rotor wear and the impact on degassing efficiency comparing the advanced Foseco pumping rotor with a simple non-pumping design and the findings help to further improve the rotary degassing process.

## 07 COATING PREPARATION PLANT



The use of a Coating Preparation Plant to improve the core coating process and foundry efficiencies.

Author/s: H. Johns, Foseco South Africa



The use of high performance coatings in the automotive foundry industry has become a necessity in order for a foundry to remain competitive in a market that demands high performance castings.

The many variables in the coating process are minimised through the use of an automated Coating Preparation Plant (CPP). This paper outlines the benefits of such a system, in which coating density is continually monitored and additions of either coating or dilutant are homogenised to ensure the product is optimally supplied for the defined application, thus ensuring that your foundry operates at maximum efficiency.

## 10 IRON TURBULENCE ANALYSIS



Iron Turbulence Analysis via Foundry Water Model I: Introduction

Author/s: Brian Pinto, Ph.D. and Brian Alquist, Foseco USA



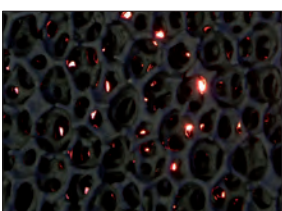
To simulate foundry casting, a bottom pour box water model was fabricated complete with actuating stopper rod and nozzle. Experiments were conducted on analogs of used and unused stopper rods along with different nozzle designs. Results indicated a number of different trends that are empirically known to be true. However, quantitatively evaluating pouring streams establishes a method to grade effectiveness of existing or new technologies designed to improve ductile iron casting. This ability to emulate customer applications in a laboratory setting significantly accelerates the learning curve when assessing potential process improvement opportunities.

## 15 CERAMIC FOAM FILTERS



Reasons for blockages in ceramic foam filters in iron and steel casting - Part 1

Author/s: Stephan Giebing and Andreas Baier, Foseco Germany



The excellent filtration efficiency and turbulence reduction properties of ceramic foam filters are generally accepted. However, filter blockages can occasionally occur and in such cases, the filter is frequently held responsible for the problem. In reality, filter related characteristics represent only a small fraction of the factors which can influence the occurrence of filter blockage.

The type and quantity of non-metallic contaminants present in the melt are a primary factor, and these are influenced by an array of foundry specific process parameters. This is the first paper in a series which will use case studies from both Iron and Steel castings to investigate the true causes of filter blockage in more detail.

# Degassing efficiency of different rotor design over rotor life



## Introduction

In order to develop the Foseco Degassing Model for simulating rotary degassing with our various rotors, Foseco had to carry out a comprehensive series of laboratory tests to measure their performance. One of the key facts which we uncovered, was that the actual shape, design and size of the rotor, all have a significant impact on the ability to remove hydrogen. On consideration of this fact, two questions immediately came to our mind:

Does each particular rotor perform well throughout the entire service life?

What is the true valuable life of a rotor, and therefore, when should a rotor be changed?

In practice many foundries replace a rotor when it becomes worn, while others continue to use it until it almost disappears. Which foundry is correct and at what point is a rotor no longer cost effective?

For an Aluminium foundry to remain competitive, productivity and cost effectiveness becomes ever more important. Quality standards need to improve continuously as reject rates are now measured in parts per million and so every stage of the production process must be carefully controlled. The target is for every stage of the process to be stable and consistent all year round and where metal treatment is concerned, there is often little chance for a second metal treatment, should the first not achieve the required specification. In order to avoid problems, the degassing parameters are normally set for the worse case conditions and so for most of the year the melt is over-degassed, wasting nitrogen, losing energy and in the most severe cases, making metal treatment the controlling factor in the foundry production rate. The greater the variation in rotor performance over service life, the more certain it is that over-degassing is required. The use of a rotor that performs equally well from Day One to the end of its service life will enable the foundry to work to closer tolerances on degassing time, inert gas usage and rotor speed.

As we considered this subject to be of such great importance Foseco decided to make a series of laboratory and foundry trials to link the scientific and practical aspects of rotor design and rotor wear.

## Rotor characterisation

The purposes of mixing are manifold, and can be summarized generically across most industries as follows [1]:

- Homogenisation
- Gas dispersion
- Suspension of solids
- Liquid-liquid blending
- Heat transfer
- Reactions

The objectives of an aluminium batch degasser can now be considered in the light of the preceding discussions of stirred tank reactors.

Hydrogen removal is still frequently the primary function of a batch degasser to remove dissolved hydrogen from molten aluminium. This is accomplished by the passage of an inert purge gas through the melt. The dissolved hydrogen seeks to equilibrate with the initially hydrogen free purge gas bubbles, which rise to the surface, carrying hydrogen out of the system [2]. The finer the gas bubbles, the greater the surface area, and the longer the residence time.

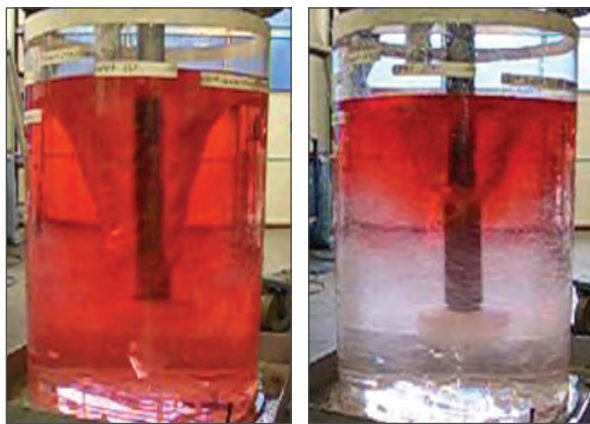
Batch degassers are also used to clean aluminium melts. Aluminium generally has a variety of non-metallic solid inclusions which can be detrimental to properties of castings [3]. Nowadays the addition of salt fluxes supports the inclusion removal. The fluxes are typically granular and entrained in the melt, for example by creating a vortex and pouring flux onto the surface or into the vortex. The flux is distributed throughout the melt, where it encounters inclusions, which become attached, and carried to the surface when the stirring stops.

Foseco favours rotors that offer a pumping action as opposed to the simpler and less effective bubble choppers offered by competitors. The pumping action of these powerful rotors draws metal from below and creates intensive mixing of the inert gas and the melt within the rotor chamber.

## Homogenizing capability of rotors in water

A well designed degassing system will have two key attributes. Firstly, the melt will be rapidly mixed to achieve and maintain chemical and thermal homogeneity throughout the process. It is important that the time required to achieve good mixing is substantially less than the metal treatment time, otherwise the applied treatment will be spatially inhomogeneous in the melt. Whilst of concern in a degassing process, this is even more problematic if the rotary system is being used for chemical dissolution (e.g. modifier or master alloy addition). Secondly, the turbulence generated by the rotor will result in a small average size of inert gas bubbles, which the well mixed flow patterns will ensure are well distributed throughout the melt. [4]

Previous water model trials and experiences from the field have shown a huge difference in mixing capability of different rotors. The pictures are taken 4 seconds after adding an ink; the FDR rotor provides an almost homogenous ink distribution whilst the non-pumping rotor result is insufficient (Figure 1):



MTS FDR rotor

Non-pumping rotor

Figure 1. Rotor operating in Perspex tank filled with water containing a red dye

Foseco has undertaken a series of experiments to further determine the mixing characteristics of different rotors under a range of operating conditions. In order to quantify the mixing behaviour, a small quantity of hot water was added to the main water tank, and a series of thermocouples located around the tank were used to log the temperature, as the tank became thermally homogeneous (figure 2).

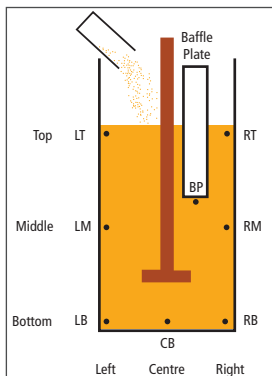


Figure 2. Locations of thermocouples in mixing tank

Various degassing rotors were attached to a Foseco degassing unit, and immersed in a water-filled Perspex tank. The same tank was used as in the previous experiments to measure rotor power [2]: diameter 60 cm, water depth ~90 cm, with the rotor positioned 20 cm above the base. The mass of water in the tank was typically 250-260 kg. A series of Type T thermocouples were located in the tank, at the locations indicated in figure 2.

For each experiment approximately 7 kg of hot water (80°C) was added to the tank once steady mixing conditions were established. Typically the addition time was 15-20 s. The complete tests ran for 1-2 minutes. A small nitrogen flow of 10 liters/minute was maintained during all tests. The average homogeneous temperature rise in the complete series of tests was ~1.3 K. The temperatures were logged at 100 ms intervals using a multi-channel Data Logger; the plotted data were normalized to compare the mixing efficiency of different rotor designs.

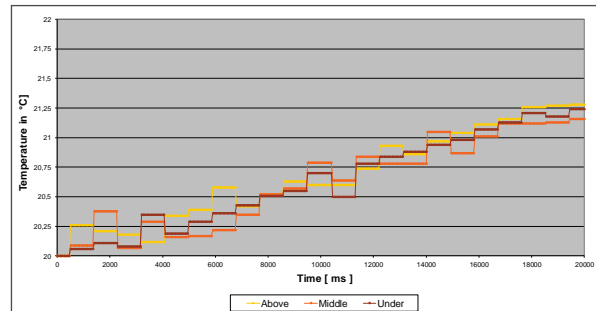


Figure 3. MTS FDR rotor – 400 rpm

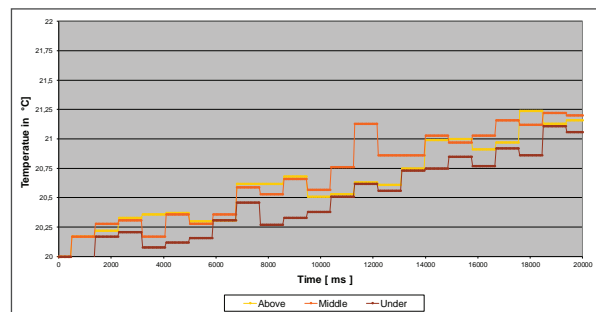


Figure 4. Non-pumping rotor – 400 rpm

The MTS FDR rotor (figure 3) – designed to give a good mixing for the MTS 1500 automated granulate addition – provides an excellent mixing. The temperature in all three measurement levels is the same almost from the beginning; the water is completely homogenized during the first 10 to 15 seconds after hot water addition.

The non-pumping rotor (figure 4) runs with the same parameters. Over the whole logging period of time the temperature in the three measurement levels varies widely. During the 20 seconds of recording the temperature, the melt is not fully homogenized.

This highly efficient mixing is of vital importance where:

- Large ladles or furnaces, with potential dead areas, are being treated
- Degassing is being carried out in a ladle where temperature loss is a concern. Fast degassing results in energy savings
- Chemical additions are being made to the melt and the stirring intensity results in higher efficiency, better yields and shorter reaction time

### Degassing efficiency of different rotor types over rotor life

Most degassing operations are not optimal, and generally rely on standard operating practices. A moment's consideration shows that a fixed, standard operating practice for a degasser, will either be wasteful, or will lead to quality variations in the final product. This is because the efficiency of the degassing process depends on a number of factors which vary from day to day, and batch to batch, such as: ambient humidity, alloy composition, incoming hydrogen level and the age of the rotor. Such variations are not taken account of in a standard operating practice.

Foseco also has a novel probe for measuring dissolved hydrogen in molten aluminium, marketed as ALSPEK\* H. One of the attractive features of ALSPEK H is its suitability for measuring degassing curves in real time, in a stirred melt purged with inert gas.

A sequential degassing experiment was undertaken to quantify the influence of the changes in rotor diameter and design over rotor service life. Before its first use, the rotors were given a standard annealing practice designed to remove residual moisture. Periodically a series of typically 3-5 degassing curves were obtained using ALSPEK H. Prior to each of these runs, the melts were either initially up-gassed with N<sub>2</sub>-H<sub>2</sub> mixed gas to a reasonable level of dissolved hydrogen, or new melt coming from the melting furnace was used.

For a better comparability, the rotor life in this study is given in a percentage of total rotor life.

All trials were carried out in a 200 kg crucible furnace with AlSi10Mg alloy at 750 °C. The rotors run at recommended rotation speed with 15 l/min nitrogen purging gas. The ambient conditions were checked on a daily base, the humidity was always between 52 and 54 % rH.

The target for degassing was 0,08 ml H<sub>2</sub> / 100 g Al.

#### MTS FDR pumping rotor

The MTS FDR high efficiency rotor is a further development of the SPR and XSR types range. An innovative design is the key for its advanced functionality, which guarantees a fast degassing and optimised melt homogenising. The trials run at 320 rpm with a 175 mm rotor diameter (figure 5 and 6).

<p>Before Trial</p>	
<p>25 % of total life time 0,08 ml H<sub>2</sub> / 100 g Al. limit reached after 230 s</p>	
<p>50 % of total life time 0,08 ml H<sub>2</sub> / 100 g Al. limit reached after 240 s</p>	
<p>75 % of total life time 0,08 ml H<sub>2</sub> / 100 g Al. limit reached after 250 s</p>	
<p>Overdue Did not reach the limit</p>	

Figure 5. FDR rotor through service life cycle

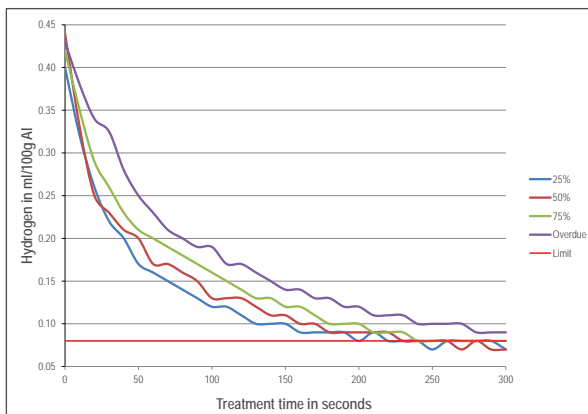


Figure 6. Degassing curves over rotor life - Fosco pumping rotor

The various FDR rotor degassing curves are very similar to each other. The degassing efficiency over rotor life decreases slightly resulting in degassing times changing from 230 seconds to 250 seconds to reach a very low hydrogen level of 0,08 ml H<sub>2</sub> / 100 g Al. In our trials the 20 seconds time increase reflects less than 10 percent change in degassing efficiency. A loss in outer diameter and more rounded edges are mostly compensated by oxidation of the graphite actually increasing the pumping chamber size, thereby increasing efficiency. The combination of design and pumping effect ensures a stable degassing behaviour over rotor service life.

All parameter settings, which are normally set during the commissioning process, with a set of consumables at the beginning of its life cycle, must take into consideration the extra degassing time required to reach the quality limits, when rotors near the end of their service life.

Moreover, the trials show that the rotor loses efficiency dramatically once its replacement is overdue. This loss in degassing efficiency is due to the critical areas of the rotor oxidizing away, particularly the bottom plate which is a major contributor to the pumping action.

Foundries should introduce a system to define the limits to a rotor change. This can be done by either a fixed treatment number or a limiting sample.

### Non-pumping rotors

Non-pumping rotors are simple bubble choppers offering no mixing and inefficient gas distribution. This can result in large untreated volumes near the bottom area of round treatment vessels. These simple rotors also find it impossible to treat rectangular or other non-round shapes. The trials were run at 320 rpm with a 175 mm rotor diameter (figures 7 and 8).

The non-pumping rotor did not reach the 0,08 ml H<sub>2</sub> / 100 g Al limit, even with variations in the treatment parameters it was impossible to degas to this level. The limit for the comparison is 0,10 ml H<sub>2</sub> / 100 g Al now.

Before Trial	
10 % of total life time 0,10 ml H <sub>2</sub> / 100 g Al. limit reached after 220 s	
36 % of total life time 0,10 ml H <sub>2</sub> / 100 g Al. limit reached after 240 s	
95 % of total life time 0,10 ml H <sub>2</sub> / 100 g Al. limit reached after 260 s	

Figure 7. Non-pumping rotor through service life cycle

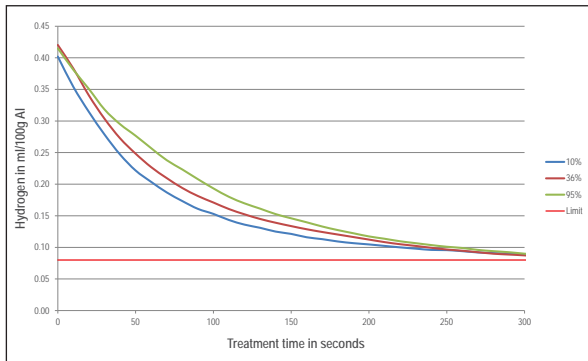


Figure 8. Degassing curves over rotor life - non-pumping rotor

The non-pumping rotor did not reach the target level of 0,08 ml H<sub>2</sub> / 100 g Al at all. The alternative limit has been achieved after 220 s with a new rotor, compared to 260 s degassing time with a used rotor. The rotor efficiency dropped by more than 20 percent over rotor service life. The simple shape of the bubble chopper rotor has no possibility to compensate the loss of the sharp edges and oxidation of the graphite will always reduce efficiency of these rotors.

Due to a 20 percent efficiency loss the treatment for new rotors must be unnecessarily extended to ensure the best melt quality over the total rotor life. The longer treatment time creates extra costs due to higher temperature loss, increased inert gas consumption and melt oxidation.

The efficiency loss is a gradual process that is very difficult for the operator to define and to recognise the right time to exchange the rotor.

## Summary

Pumping is better than non-pumping because of better melt mixing. Offering improvements in metal quality, consistency and a reduction in cost per treatment.

Rotors lose efficiency over rotor life, but depending on the design, the loss can be less than 10 % for the FDR and more than 20 % for very simple designs.

The efficiency loss must be added to the treatment time for new rotors to reach the limit throughout their life, but this extra time costs money.

It's important to define a maximum rotor life, either by a fixed number of treatments or by use of limiting samples.

## References

- [1] R.R. Hemrajani and G.B. Tatterson, in "The Handbook of Industrial Mixing", editors E.L. Paul, V.A. Atiemo-Obeng and S.M. Kresta, Wiley Interscience (2004)
- [2] G. K. Sigworth and T. A. Engh, Met. Trans. B 13(3), p447 (1982).
- [3] R. J Anderson, Metallurgy of Aluminium, H.C Baird and Co.(1930).
- [4] M. Zlokarnik, "Stirring: Theory and Practice", Wiley-VCH, Weinheim (2001).
- [5] The technology of batch degassing for hydrogen removal from aluminium melts using different rotor designs, Foundry Practice 256

## Links

Scan this QR code with your smartphone to view a video relating to this paper.



Mixing capability of different rotor designs in a Perspex tank filled with water

# The use of a Coating Preparation Plant to improve the core coating process and foundry efficiencies



## Coating Preparation Plant (CPP)

There is a continuing requirement for foundries to manufacture increasingly complex, high performance castings - while driving down production costs. A significant proportion of production costs can be attributed to re-work due to surface defects and these can be eliminated or significantly reduced through the use of the correct refractory coating.

The choice of coating is specific to the metal / mould interactions that are to be overcome, and the rheological properties can be tuned to the application requirements, however a coating will only achieve optimum performance when it is applied at the correct layer thickness. If the layer thickness is too thin, the coating will not provide adequate protection and if it is too thick there is the risk of scabbing defects, the formation of runs and drips and the cost penalty of using too much coating. The layer thickness of the applied coating can be controlled by diluting the as supplied coating, with a higher dilution resulting in a reduced layer thickness. Therefore, variations in dilution through poor process control and measurement, will lead to variations in applied layer thickness, resulting in variations in surface finish, defect levels and re-work costs. Traditionally coating dilution has been controlled through intermittent measurements of the diluted product using viscosity cups or Baume, however the intermittent nature of these tests and the dependence on an operator to interpret results and ensure the coating is homogenised after dilution, inevitably leads to application variations.

These variables can be minimised by the application of an automated Coating Preparation Plant (CPP), and this paper outlines the benefits of such a system in which coating density is continually monitored, and additions of either coating or dilutant are added and homogenised to ensure the product is always optimally supplied for the defined application. The CPP has been developed specifically for metal-casting operations by ProService Srl and is distributed exclusively by Foseco International Ltd.

The CPP is designed to accommodate a wide range of application methods including spray, dip and over-pour, and can be connected to all major packaging systems from drums to bulk silos. The CPP can be configured to work automatically, manually or intermittently dependent on the foundry process

Features and benefits of the CPP include:

- Continuous monitoring (independent of operator)
- Controlled layer thickness
- Reduced coating consumption
- Optimised drying
- Fewer scrap cores/moulds
- Reduced casting scrap and defects attributed to poor coating practice
- Improved traceability and quality control
- Reduced risk of coating contamination and bacterial attack
- Improved working environment – specifically the handling of solvent based coatings
- Improved productivity
- Reduced casting manufacturing costs
- Improved profitability

## Introduction

Atlantis Foundries (Pty) Ltd is a major South African and international truck engine block producer with an output of 68,000 tonnes of grey iron per year.

The company is a wholly-owned subsidiary of Mercedes-Benz South Africa and part of the Daimler group and is the leading automotive foundry in the country.

Atlantis Foundries' plant is located in Atlantis, approximately 50 km north of Cape Town along the west coast of South Africa.

Atlantis Foundries have been using Foseco products for the past thirty years.

The engine blocks that are produced at Atlantis Foundries are primarily shipped to America and Europe with a smaller number being shipped to other parts of the world.

Being an international player in the automotive industry, Atlantis Foundries strives to keep abreast with all available technology. Foseco South Africa saw the need for Atlantis Foundries to take advantage of the available technology on offer from Foseco and thus entered into discussions with Atlantis management and engineers regarding the optimisation of their coating application. Foseco proposed the Total Coating Management Concept which would enable Atlantis Foundries to achieve the highest standards possible in coating technology.

## Atlantis foundries background to CPP installation

Foseco first approached Atlantis in:

- 2007: First proposal for CPP given to Atlantis Foundries
- 2009: Due to economic recession the project was placed on "hold"
- 2010: Project to convert from solvent based to water based coating started
- 2011: Proposal for a dual solvent & water based CPP given to Atlantis Foundries
- 2012: Atlantis placed order for the CPP and dip tank
- 2013: CPP and dip tank installed and commissioned by Pro Service / Foseco in January 2013

Prior to the CPP installation

- Coating control using manual flow cup viscosity
- Flow cup viscosity reading was operator / cup dependant
- Manual dipping
- Difference in wet film thickness depending on flow cup viscosity and dipping time
- Coating related scrap

Atlantis Foundries used viscosity as their main control for the coating but it can be shown that this can be influenced by a number of variables.

Example: the viscosity control specification is normally not re-adjusted in the cooler or warmer periods of the year. However, the viscosity is highly influenced by temperature, and without compensation the result will be a difference in the final layer thickness applied, which then impacts on the casting output efficiency.

This limitation can now be overcome: The Coating Preparation Plant (CPP) automates the coating preparation from its supplied state through dilution to a defined specific density and subsequent control and monitoring on a continuous basis to ensure the consistency of the application.

By converting the applied control measures from viscosity to density, variables such as temperature are eliminated, because the solids content of the coating is kept constant and the product application consistency is lifted to a new level of quality.

After CPP installation

- Coating controlled by CPP using "Density Sentinel" probe
- Constant density readings (3 decimal places)
- FANUC Robot Dipping
- Constant wet film thickness readings
- Decrease in coating related scrap

CPP configuration

- Coating storage tank: 2000 litre capacity
- CPP tank: 560 litres preparation tank supplying coating via diaphragm pump to dip tank
- CPP fitted with both "Density Sentinel" and "Viscosity Sentinel" systems
- Dip tank: 2200 x 1200 mm x 1000 mm high and fitted with a swing arm
- Coating runs via gravity back into coating collection tank and using a diaphragm pump, it is pumped back to CPP preparation tank
- In-line modular filters are installed to remove sand deposits from the coating and protect the CPP equipment



Figure 1. FANUC robot dipping

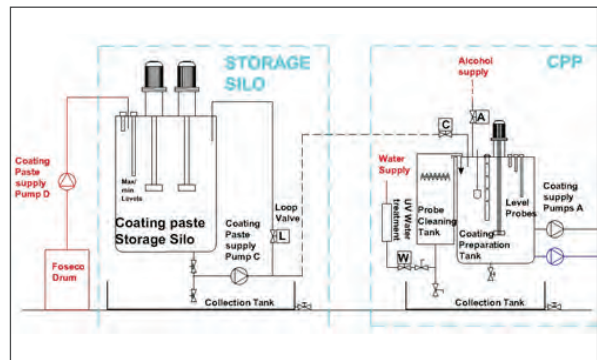


Figure 2. Functional scheme of the storage tank and CPP tank

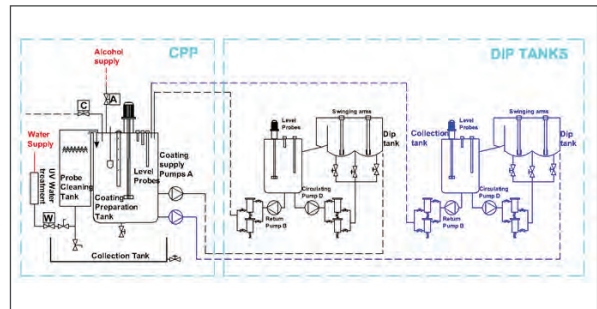


Figure 3. Functional scheme of the CPP tank and dip tank



Figure 4. Holding tank and filters.



Figure 5. Panel, storage tank and preparation tank on the right

## Coating Application Consistency The Total Coating Management Concept

Foseco, together with its partner ProService have developed a stand-alone system which utilises the accuracy of density measurement to control coating consistency prior to application.

The Density Sentinel probe has been developed to operate effectively in the core shop and moulding line environments of a foundry.

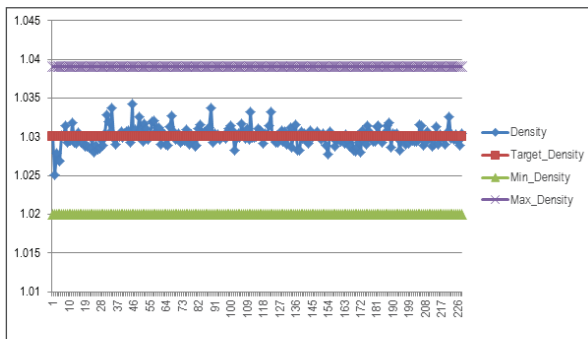


Figure 6. Illustrating the maximum and minimum targets for density

As illustrated in the graph above, the applied wet layer thickness will be consistent as the coating density is maintained within the specified limits and controlled closely around the target specification. This is because the measurements are continuous and not open to operator interpretation, which can lead to inaccuracies that will lead to poor coating application and increased cleaning/fettling and scrap costs.

Coating application consistency was also improved by the introduction of robotic dipping which provided controlled dip times and core manipulation. When the CPP was first installed the density range was set to between 1.1% and 1.5%, this was subsequently reduced to between 1.02% and 1.03%, indicating that the density can be controlled to a very high tolerance.

The CPP design was adapted to the specific requirements of Atlantis Foundries, in that it:

- Reacts immediately to the coating density changes, ensuring a continuous control of the coating density. It should be noted (Figure 3) that over a 24 hour period the Density Sentinel has conducted 226 tests and adjustments to the coating were made when required
- The unit is fully operator independent, ensuring manual input does not affect coating consistency
- It is possible to measure the coating density at the required depth (for example, in the case of the dipping application of cores: it is important to verify that the coating density value does not alter according to the dipping depth)
- The Density Sentinel is not affected by the turbulent flows inside the tank
- The measurement has a very high level of precision (three decimal points)
- The new Density Sentinel Plus allows for the creation of databases, to calculate statistics and to monitor the entire coating shop from one or more stations

Coating Preparation Plants have been installed by Foseco at many foundry locations globally and have been shown to deliver consistent coating dilution, eliminating variability of coating application and reducing subsequent casting defects and scrap associated with poor coating practice.

## Conclusion

As the demand for more complex, critical castings increases, the higher quality standards are set, the function and performance of the coating utilized in the foundry process becomes critical. For example, the impact of a high performance core coating on the overall production cost of a typical automotive foundry can be significant, allowing foundries to reduce their fettling, cleaning, and casting inspection operations.

The coating cost is typically a fraction of the total manufacturing costs and usually would be less than 1% of total production costs.

For Atlantis Foundries to maintain a competitive edge within the foundry automotive market and their need to produce increasingly complex, higher quality castings, at increased production levels and with lower overall costs, they had to get the competitive edge by investing in a CPP to optimise the coating preparation and to ensure the consistency and quality of the components being cast.

## References

- Foseco Ferrous Foundry's Handbook
- ProService Technology for foundry solutions.
- Atlantis Foundries



## Introduction

There are obvious differences between water and molten metal; most notably density and surface tension. However, dynamic water modeling has become a universally accepted method for observing and evaluating turbulence of steel melts in and around steel mill tundish ladle systems. Partial-to-full scale models are commonly used for this purpose. Notable achievements resulting from water modeling are tundish grade transition and ladle draining yield increases, as well as overall metal quality improvements resulting from turbulence control in the tundish and mold. Up to several million dollars per year are saved via operating efficiencies arising from solutions derived using sophisticated water modeling experiments. Most commonly, these are undertaken by industry suppliers or engineering companies with expertise in the field [1].

There are many opportunities to improve casting yield in ductile iron foundries [2][3]. Among these are methods recommended to reduce turbulence in foundry metal casting and thus increase the relative cleanliness of iron melts, particularly in ductile iron where oxidation and slag formation are prone [4]. These phenomena are major contributors to defects commonly found in castings [5]. Though this may be obvious, the potential for significant foundry cost savings arising from such turbulence reduction efforts is less clear. Direct observations around the automatic pour box nozzle during casting and late stream inoculation suggest that a genuine opportunity for improvement exists.

Experience dictates that the effectiveness of automatic pouring is strongly influenced by the gradual build-up of slag and other impurities on the stopper rod and inside the bore of the ductile iron pouring nozzle [6]. To better understand the complex relationship between pour box, stopper rod, nozzle and iron stream, a workable model is needed; one that simulates casting of molten metal in a controlled environment. If an understanding is developed as to how stopper rod and nozzle condition and geometry affect metal flow into molds, two things can be achieved:

1. Validation of usage recommendations regarding existing product designs.
2. Development of improved products that mitigate shortcomings associated with current designs.

By combining aspects of water modeling and optical sensing it has become possible to evaluate the effects of stopper and nozzle conditions in a typical automated ductile iron pour box. In order to reproduce and quantify these effects, a full-scale water model of a typical bottom pour box system was fabricated. A quantitative stream turbulence measurement system was designed and constructed using specialized optical sensing and data acquisition software systems.

## Background

### Water Model

A full-scale foundry pour box was constructed using plexiglass. Figure 1 is a detailed schematic and Figure 2 shows a photograph of the assembled model. The pour box is fitted with a replica stopper rod and nozzle, fabricated out of plastic. Maximum capacity is approximately 280 liters (75 gallons) of water, which simulates a pour box filled with 1950 kg (4300 lbs.) of iron. A blue dye is added that renders the water opaque, allowing detection by the optical stream evaluation equipment. A manually-operated actuation mechanism is used to seat and unseat the rod in the nozzle to simulate openings and shutoffs during casting. The design is such that different stopper rods and nozzle designs can be easily interchanged. The water model can be used as stand-alone equipment for evaluation of flow inside the pour box or coupled with optical sensing equipment to quantitatively evaluate the turbulence of the liquid stream as it exits the nozzle.

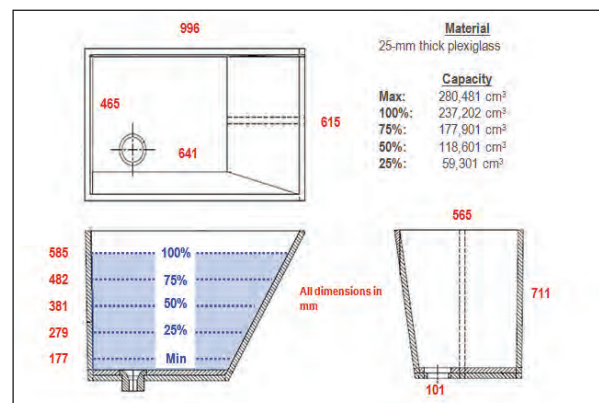


Figure 1. Schematic of bottom pour box water model with additional details

## Stream Analysis

A novel technology for observing and measuring metal stream turbulence has been developed. Originally conceived as a tool for use with late-stream inoculation, it was upgraded to quantify metal flow quality using proprietary mathematical algorithms to define turbulence of a metal stream in-situ. The hardware for this system consists of a high-speed digital camera and laptop computer that runs the software. It was further upgraded to quantify the same characteristics of a water stream to be used with the foundry water model. Figure 3 shows photos and screen-shots from the stream analysis software.

The output of the algorithm is a measure of flow turbulence from the nozzle, a function of the stream geometry. The software is able to analyze the dynamic changes of the pouring stream during casting by taking a series of high speed images and grading their shape with respect to a completely laminar stream. The output is laminarity index (LI), an average value of the geometric stream deviation from ideal (100% laminar flow). A higher LI number (range: 0 – 100) indicates a more laminar flow. A key attribute of this system is its automatically triggered measurement of laminarity index to generate data that grades every casting individually. The equipment can be set up in a foundry and record data from each casting for extended periods of time without an operator.

It is known that as a stopper rod and nozzle are used in a ductile iron bottom pour box, performance decreases with time due to wear, slag buildup, and other mechanisms. In an automated casting line where thousands of castings are made per day, degradation of the iron flow control system can directly lead to casting defects. Turbulence entrains air and slag, which can lead to oxide films, bubbles and other undesirable defects in the castings. Stopper rods and nozzles are commonly replaced when they have exceeded their useable life on this basis; however the criteria on which this is judged is often subjective. The optical system can continually monitor the situation and quantify stream turbulence, generating trendlines that can be used to establish process control limits. Knowing the optimum time to replace a stopper rod or nozzle is one way to reduce rejected or reworked castings.

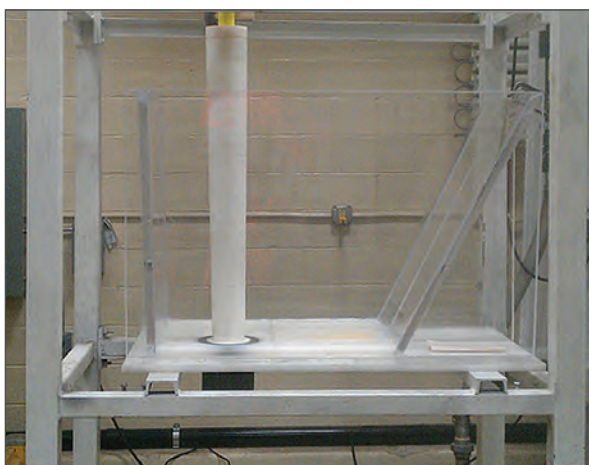


Figure 2. Photograph of bottom pour box water model with stopper rod and nozzle replicas installed

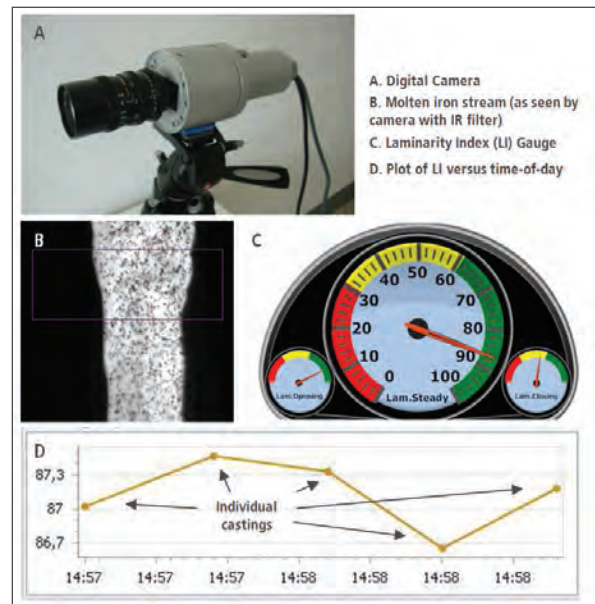


Figure 3. Digital camera and screen shots from the software that illustrate the algorithm outputs are shown

Having a water model that accurately simulates the action of a foundry flow control system allows for not only characterization of liquid flows using current stopper/rod technologies, but also serves as a tool for fundamental understanding of the relationships between the working parts within a foundry pouring system. With this knowledge, novel products can be developed to meet customer needs on an application-specific basis. The water model can then serve as a proving ground for new pour box, stopper rod, and nozzle designs in a low-risk environment where the outcomes are relevant, meaningful, and can incorporate using tools such as precision stream analysis instrumentation.

The first steps in this process are to investigate common features and conditions within a foundry bottom pour box with respect to stream quality. Using the stream analysis system in tandem with the water model produces quantitative data that otherwise could not be generated by either piece of equipment separately. The introduction of both systems and the preliminary experimental results serves as the basis for this paper.

## Experimental procedures

### Laboratory Setup

Figure 4 shows a schematic and a photograph of the experimental setup. As shown, a camera is positioned about 1.5 meters away from the water model, aimed at the water stream as it exits the nozzle opening. The stream is back-lit using a high-powered lamp and a piece of translucent plastic to create strong contrast between the stream and background required by the optical system. Below the nozzle is a catch-basin for the expelled water.

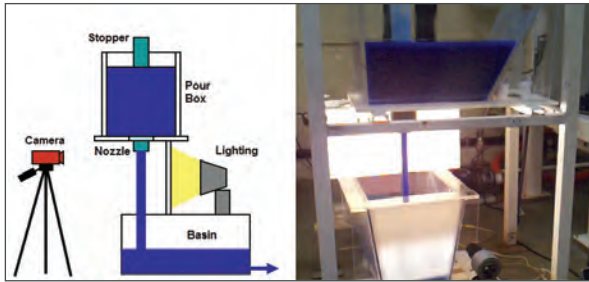


Figure 4. Schematic (side view) and photograph of experimental setup are illustrated

### Stopper Rods and Nozzles

Figure 5 shows drawings of stopper rod and nozzle patterns selected for the preliminary experiment, those commonly paired with this bottom pour box design. A typical bore configuration is a cylindrical hole. One of the more uncommon features, a “cross-bore,” was also selected because its design is claimed to improve the flow of iron through the nozzle. Its effectiveness was derived through field trials but not using any devices to actually quantify the results.

Figure 6 shows replicas of the stopper rod and nozzles. These were made using fused deposition modeling (FDM) technology to render full-scale copies of the refractory parts in plastic. Used replicas were reverse-engineered from used specimens taken from foundries using laser scanning in combination with FDM techniques. Figure 6 (B, C) includes a comparison between the actual used stopper rod and its plastic replica.

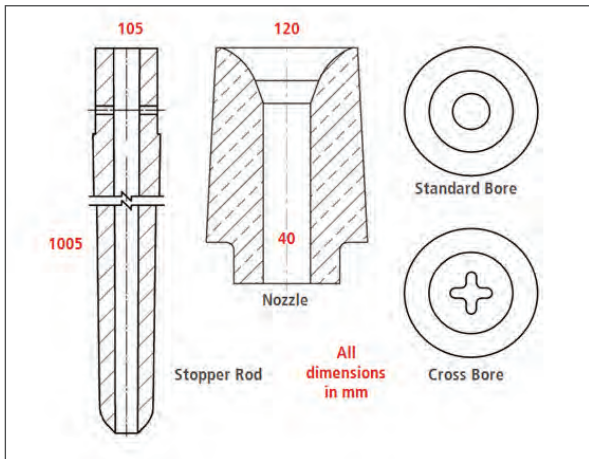


Figure 5. Diagrams of stopper rod and nozzle patterns selected for preliminary testing

### Parameters

To investigate the effect of stopper condition and nozzle design on stream quality, used and unused stoppers were coupled with both nozzle designs (standard and cross-bore) for a series of tests. It was also theorized that pour box fill height may have an effect on stream quality due to potential influence of differing volumes of liquid on flow rate. To evaluate this, four different box fill height intervals (25%, 50%, 75%, and 100% working capacity - ref. Figure 1) were

evaluated per stopper/nozzle configuration. With the optical system collecting the stream laminarity data, a series of three repeat tests were conducted per fill level per rod/nozzle pairing for a total of 48 raw data points. The stream analysis system also collected still images from each acquisition; these were visually analyzed for comparison. This serves as a secondary check to ensure numerical outputs of the algorithms are a reasonable representation of the actual outcomes.

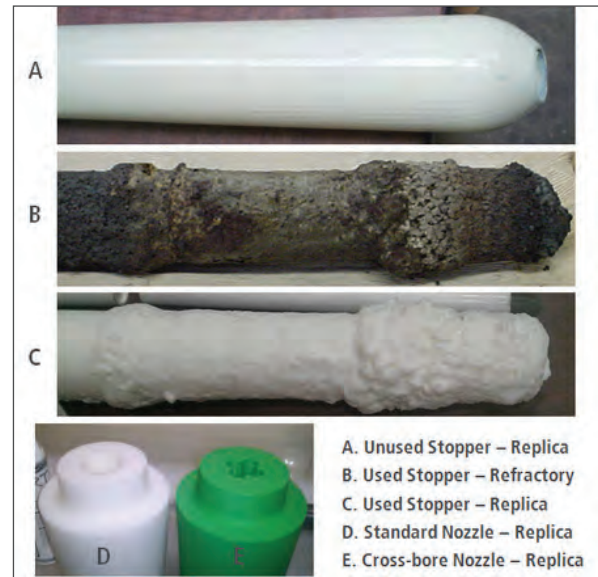


Figure 6. Photographs of plastic replica stopper rods and nozzles used in the experiment. 6B is the actual refractory piece from which the replica (6C) was derived

### Results and discussion

Table 1 lists results of the first round of trials. Shown are averages and standard deviations for each test. The first noticeable result is that the fill height of the pour box does not appear to influence the stream quality for a given stopper/nozzle configuration. Where the unused stopper was tested, the average values are within one laminarity index (LI) unit. There is slightly more scatter in the results for the used stopper, but this is an effect of higher standard deviations in the overall test data caused by its irregular geometry. These results may differ in a foundry because, due to density differences, metallostatic pressure exerted by iron is about seven times higher than water. Also, the water in the pour box was still prior to each test; a turbulent state may have also influenced the outcomes differently.

When the standard nozzle was used, there was a large measurable effect of rod condition on laminarity index. The used stopper caused a more turbulent stream to exit the same nozzle that produced a very laminar flow with an unused stopper. An explanation for this is that the buildup on the used stopper causes the fluid to swirl and change directions as it passes the irregular stopper rod surface, becoming more turbulent. The asymmetric shape of the stopper causes the fluid to enter the nozzle at unstable velocity, which causes the stream exiting the nozzle to also be turbulent and fan out. Figure 7 shows photographs and a schematic that illustrates what is occurring.

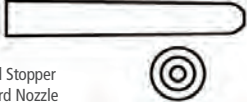
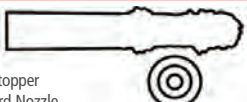
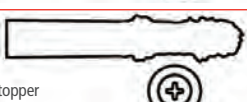
	Fill Level	Laminarity Index (LI)			Average	Std. Dev
		Exp. 1	Exp. 2	Exp. 3		
 Unused Stopper Standard Nozzle	100% to 75%	92.29	92.73	92.78	92.60	0.27
	75% to 50%	92.12	92.11	92.15	92.13	0.02
	50% to 25%	92.67	92.70	92.63	92.67	0.04
	25% to Min	92.74	92.80	92.18	92.57	0.34
 Used Stopper Standard Nozzle	100% to 75%	79.33	75.86	79.82	78.34	2.16
	75% to 50%	80.43	79.76	80.81	80.33	0.53
	50% to 25%	82.21	81.75	79.63	81.20	1.38
	25% to Min	81.69	83.74	83.59	83.01	1.14
 Unused Stopper Cross Bore Nozzle	100% to 75%	91.55	91.28	91.57	91.47	0.16
	75% to 50%	91.52	91.68	91.69	91.63	0.10
	50% to 25%	91.01	91.55	90.45	91.00	0.55
	25% to Min	90.63	90.24	90.76	90.54	0.27
 Used Stopper Cross Bore Nozzle	100% to 75%	81.04	88.95	84.81	86.88	2.93
	75% to 50%	88.29	87.71	89.88	89.30	2.24
	50% to 25%	82.39	84.71	81.51	83.11	2.26
	25% to Min	88.30	83.58	85.85	84.71	1.61

Table 1. VISION data from testing under different experimental conditions

Testing with the cross bore nozzle produced slightly different results. The unused stopper rod resulted in a high level of laminarity as with the standard bore. However, when the used stopper rod was tested the laminarity index was lower, but only by 5 units (91 to 86), compared to a decrease of 12 units (93 to 81) during the same tests using the standard nozzle. What appears to be occurring is that turbulence generated around the used stopper rod is being suppressed by the cross-shaped bore (due to geometry) and the resulting stream takes on a more laminar appearance. This is illustrated in Figure 8, which depicts representative images from the four different stopper/nozzle configurations. What is apparent is that the used rod generates turbulent flows from both nozzles, but the pouring stream is more laminar exiting the cross bore nozzle. Implications of this are as a rod collects build-up, negative effects on stream quality are greatly reduced when a cross bore nozzle is used.

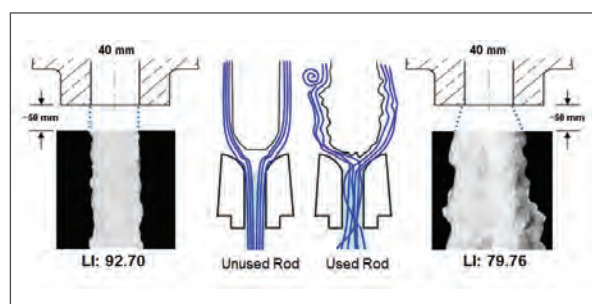


Figure 7. Stream photos captured by optical system with schematics of two different rod/nozzle combinations

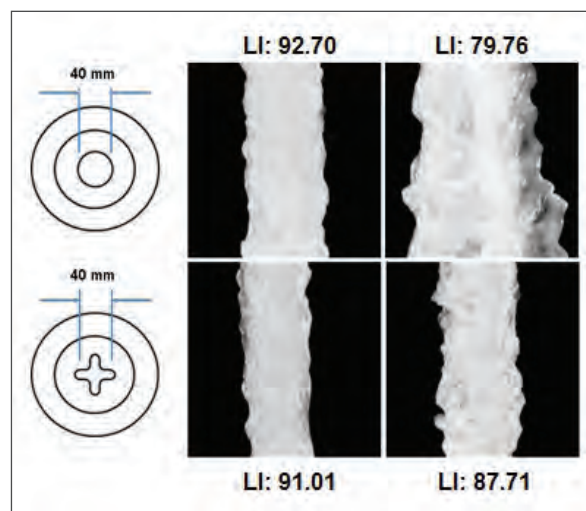


Figure 8. Representative stream photographs of different stopper/nozzle configurations tested.

Based on the preliminary round of testing, there were at least three significant findings:

1. Pour box capacity does not appear to influence the stream quality when the fluid is water and in a generally static condition prior to casting. Simulation of ferrostatic pressures is needed.
2. The cross-bore nozzle and unused rod pairing doesn't necessarily improve the stream quality beyond that of a standard bore nozzle. Approximately the same laminarity index was measured for both.
3. When the cross-bore nozzle is coupled with a used rod, the stream was significantly less turbulent when compared to the same rod with a standard bore nozzle.

The combination of a foundry water model and optical sensing technologies has produced a system capable of measuring significant changes to stream characteristics and quantifying them with a laminarity index. Results are repeatable and there is a visual aspect to test results that is a valuable tool for comparing numerical stream quality data to something relatable to customers. The laboratory water model can be used as a testing ground for novel concepts in stopper rod and nozzle design. Since the stream analysis system is configured for use both in foundries and the laboratory, any prototype parts evaluated in the laboratory for flow behavior can be trialed in the field (and vice versa), analyzed using the same equipment.

### Summary

A full-scale water model was constructed as a means to simulate different conditions present in ductile iron casting operations. Different stopper and rod patterns were interchanged in the model allowing for evaluation of the pouring stream turbulence as a function of design. The model was outfitted with a novel optical sensing system, capable of quantifying stream quality with a laminarity index value for each pour. Preliminary testing of new and used rod replicas showed that turbulence generated by a used rod negatively affected flow out of a nozzle even if it was pristine. By changing the nozzle bore to a cross-bore shape, the turbulence at the nozzle exit was reduced significantly. These findings are preliminary but serve as an example of the strong potential capabilities of this system. The water model and optical sensing system represent a novel pairing of equipment that can be used to effectively trial flow control design concepts in the laboratory in full scale, quantify the results in an unprecedented way, and get an accurate impression of how effective they will be in the field.

### Acknowledgments

The authors would like to acknowledge their respective companies for the resources provided and the opportunity to publish this work. Special thanks are due to Mr. Thongxai Vouthy, flow simulation technician with Vesuvius plc, for data collection and maintaining the foundry water model. We also wish to thank Mr. John Rogler (Vesuvius plc), Mr. Douglas Spoonley (Foseco), and Mr. Tommaso Todescan (ProService Technology) for their expertise and insight on the subject material.

### References

1. Watermodelling, [www.vesuvius.com](http://www.vesuvius.com).
2. Rizzo-Downes, N.T., "Ten Steps to Improving Casting Yield in Ductile Iron Foundries", *Ductile Iron News*, Issue No. 3 (2005).
3. Brown, John R. *Foseco Ferrous Foundryman's Handbook*. Oxford: Butterworth-Heinemann Publishing, 2000.
4. Uren, G.L., "Automatic Pouring of Treated Ductile Iron", *AFS Transactions*, pp. 347–352 (1980).
5. Kaczmarek, E.R., Leitermann, R., Heine, R.W., "Pinhole and Slag Casting Defects in Ductile Iron Processing", *AFS Transactions*, pp. 67 – 75 (1997)
6. Andree, W., "Automatic Pouring With Stopper-Controlled Pouring Mechanisms", *Proceedings of International Iron Melting Conference – Orlando* (2003).

### Additional resources

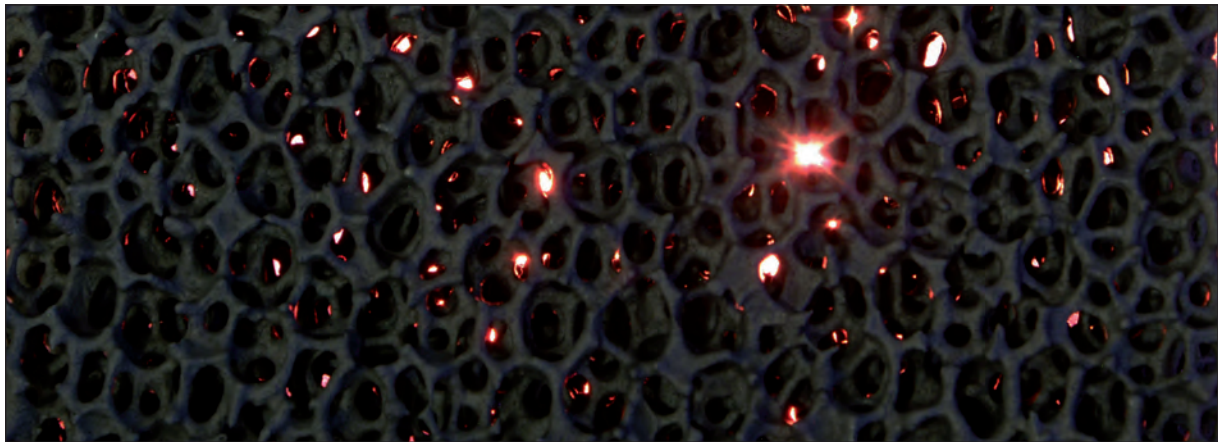
[www.foseco.com](http://www.foseco.com)

[www.vesuvius.com](http://www.vesuvius.com)

[www.proservicetech.net](http://www.proservicetech.net)

This paper was originally published in the Proceedings 2013 Keith Millis Symposium on Ductile Iron by the American Foundry Society, copyright 2013 ([www.afsinc.org](http://www.afsinc.org)).

# Reasons for blockages in ceramic foam filters in iron and steel casting – Part 1



## Introduction

The use of ceramic foam filters in the industrial production of cast products represents current state-of-the-art technology. This is partly due to their very good filtration efficiency and ability to separate the non-metallic contaminants from the molten metal. In addition, the turbulence reducing effect of the filter limits the degree of re-oxidation of the molten metal. Occasionally, however, filter blockages occur. In the absence of an exact analysis to determine the cause, the filters involved are frequently deemed to be primarily responsible for these processes. In many cases, a cooperative effort with the foundry leads to the discovery of the true causes and allows suitable remedies to be adopted.

## The problem

In addition to reducing turbulence the main purpose of using ceramic foam filters is to separate non-metallic contaminants from the molten metal. As a result of this, the open cross-section of the filter medium decreases continually throughout

the pour. Depending on the type and quantity of non-metallic contaminants that are to be removed from the molten metal via the filter, this process can result in the filter becoming blocked. This is reflected in the casting results in the form of increased pouring times, cold lapping or incomplete casting. Generally, such processes depend on the respective flow rate in each specific case and they exercise a direct influence on the capacity of the filter medium. With regard to the flow rate and capacity of ceramic foam filters, the following characteristics exert an influence:

- type of ceramic
- weight
- porosity
- filter surface area
- filter thickness
- flow rate

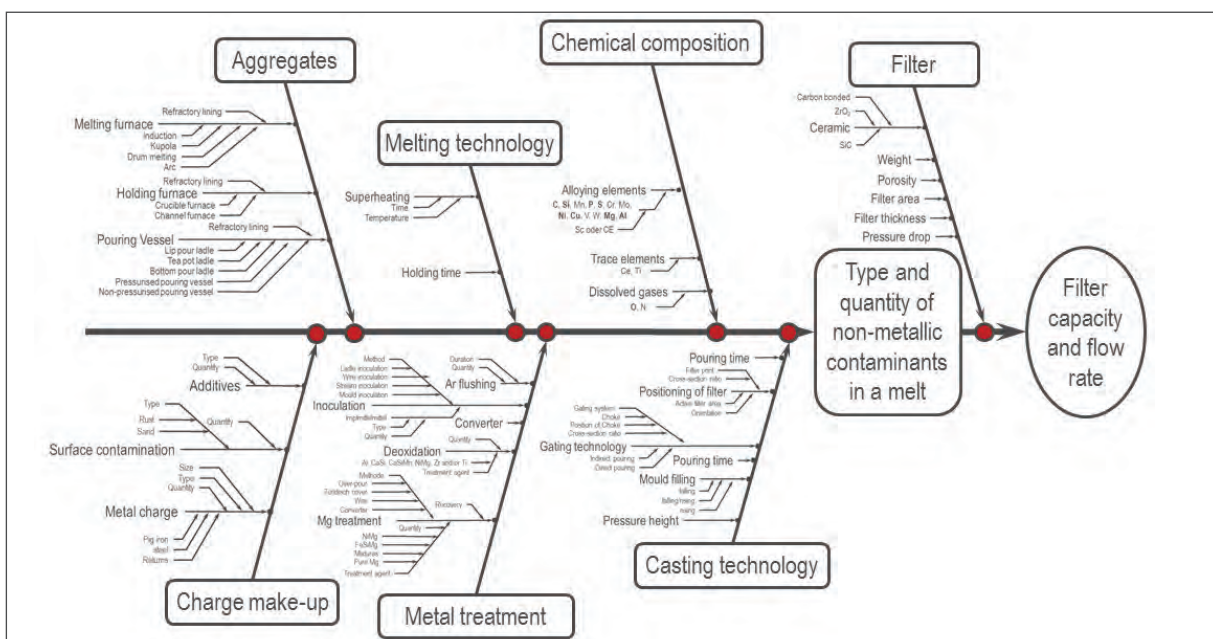


Figure 1. Cause/effect diagram for filter capacity and flow rate in Iron and Steel castings

In many cases, however, the process of analysing the causes of filter blockages is significantly more complex. From the point of view of failure prevention, the analysis and investigation should not be restricted to the characteristics of the filter medium used. The filter-related characteristics mentioned above represent only some of the factors which need to be considered. The type and quantity of non-metallic contaminants in the melt are influenced by a large number of foundry-specific process parameters, and they are difficult to quantify. These process parameters can be categorised into the areas of charge make-up, aggregates, melting technology, metal treatment, chemical composition and casting technology (Figure 1).

In the course of this publication series, case studies from both iron and steel castings will be used in order to discuss the causes of filter blockage in more detail. The following example is concerned with the occurrence of filter blockages during the production of carbon and low alloy steel castings using the direct pouring method.

### Case study

During the production of castings in carbon and low alloy steels, using the direct pouring method, STELEX\* PrO filters used were prone to irregular blockages. The casting weight range was 360-560 kg. The filters that were first used were STELEX PrO Ø150x30 and Ø175x35 10 ppi. The problem was initially addressed and remedied through the use of larger filters.

The melt shop of this foundry has several medium frequency induction furnaces providing a maximum capacity of 2.5 tonnes each. The refractory lining of the furnaces and ladles consisted of a spinel forming material (approx. 85%  $Al_2O_3$ , approx. 12% MgO). The bottom pour ladles used had a nozzle diameter of 50 mm. The de-oxidation of the steel was carried out during tapping into the ladle using an addition of 0.06% aluminium. The great majority of castings were uncored and produced in green sand moulds.

### Preparation of the casting trials

When this study was carried out, the castings were poured with STELEX PrO Ø175x35 and Ø200x35 10 ppi filters. In order to investigate the influence of the filter upon blockage, the bulk density and pressure drop of each filter was measured prior to casting. The bulk density was determined in accordance with BDG [Federation of the German Foundry Industry] Directive P100 [1]. The physical principles behind the method for calculating pressure drop values in ceramic foam filters are described in [2]. Figure 2 shows a schematic diagram illustrating how the measuring equipment works. The device used to determine the pressure drop sucks in air at predetermined capacity levels through the filter. Due to the special design of this measuring equipment, the suction capacity gives rise to negative-pressure within the system. The pressure drop is given by the difference between the ambient air pressure and the air pressure within the system. Introducing a filter causes the negative pressure within the system to increase. Generally, the larger the pressure drop caused by a filter, the lower the throughput of the filter.

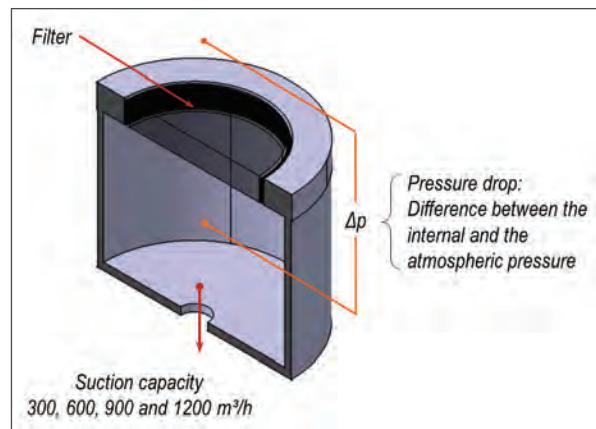


Figure 2. Determination of pressure drop caused by a filter - schematic illustration of the way the measurement equipment works

Figure 3 shows the relationship between pressure drop and the suction capacity, using STELEX PrO Ø175x35 and Ø200x35 10 ppi filters as examples. The STELEX PrO Ø175x35 10 ppi displays greater pressure drop compared with STELEX PrO Ø200x35 10 ppi with equal suction capacity. This difference can be explained mainly by the fact that the filters have different surface areas ( $240.5 / 314.2 \text{ cm}^2$ ). Figure 3 also shows that the pressure drop for the STELEX PrO Ø175x35 10 ppi with a suction capacity of 900  $\text{m}^3/\text{h}$  corresponds to that of the STELEX PrO Ø200x35 10 ppi at 1200  $\text{m}^3/\text{h}$ . This behaviour can be used in casting tests designed to enable comparison of the flow rate capacity of different filter sizes. Figure 4 shows an overview of the bulk density-dependent pressure drop values measured during these tests.

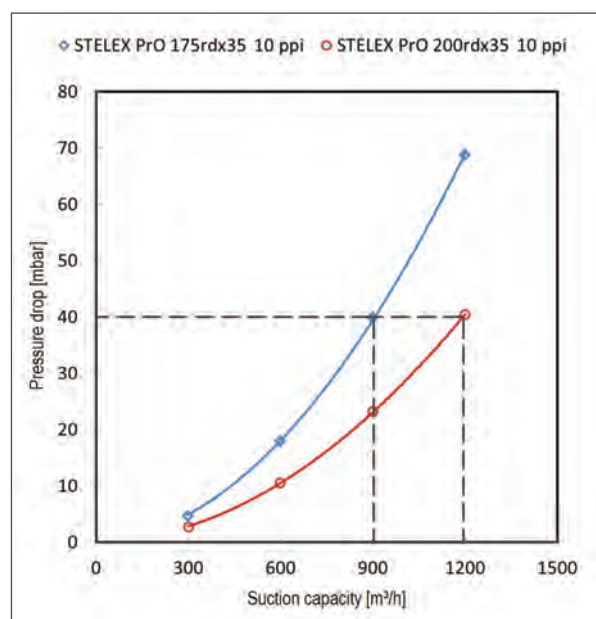


Figure 3. Pressure drop of STELEX PrO Ø175x35 and Ø200x35 10 ppi filter samples in relation to the suction capacity

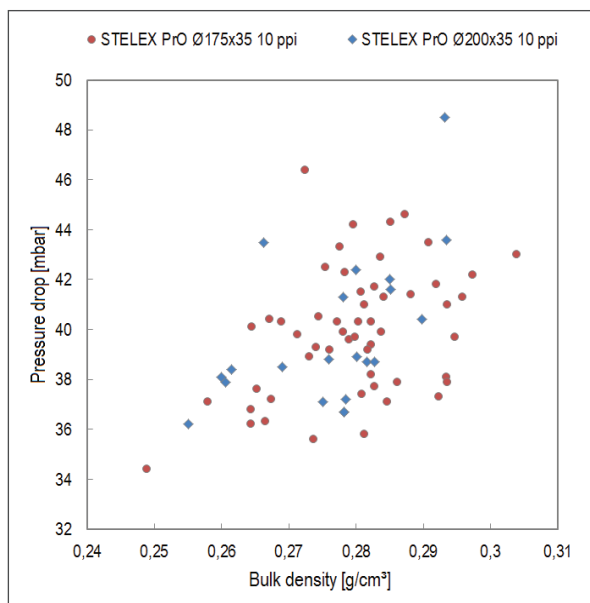


Figure 4. Pressure drop of STELEX PrO Ø175x35 10 ppi (900 m<sup>3</sup>/h) and Ø200x35 10 ppi (1200 m<sup>3</sup>/h) in relation to the bulk density

## Test procedure

Initially, the tests involved pouring 41 castings of similar type (A to C) using 9 melts of low-alloy steel (G 35 CrMoV 10 4, G 42 CrMo 4 and G 30 NiCrMo 14); all castings were produced with STELEX PrO Ø175x35 10 ppi filters. No problems or issues were noted during the trial. The specific filter capacities ranged from 1.50-2.26 kg/cm<sup>2</sup>. The bulk density of the filters used ranged from 0.249-0.304 g/cm<sup>3</sup>. The pressure drop values ranged from 34.4-46.4 mbar.

In the next stage, a series of castings (D) were poured using three batches of GS-52.3, each part filtered with one STELEX PrO Ø200x35 10 ppi. These castings had a net weight of 454 kg and a poured weight of 560 kg. The specific filter capacity of the filters was 1.78 kg/cm<sup>2</sup>. This corresponds with the mean levels obtained in the previous tests. In terms of bulk density and pressure drop, the filters provided figures of 0.260-0.290 g/cm<sup>3</sup> and 36.7-41.6 mbar. Whereas in the first batch three castings were poured without any problems, filter blockages were observed in a total of four moulds during the two successive batches.

The initial assumption was that these blockages occurred due to the use of filters with higher densities and/or high degrees of pressure drop. The results obtained so far did not confirm this assumption. Those filters that became blocked during use were of average or low bulk density and the pressure losses were medium to low.

A further assumption was that the filter blockages were caused by low flow rates for the alloy GS-52.3. However, previous comparative studies of fluidity characteristics carried out by the foundry on GS-52.3 and G 42 CrMo 4 using lattice samples, showed they had very similar fluidity. It may therefore be assumed that the alloy element content of the materials under investigation exercised only a minor influence.

The filters that became blocked were subjected to thorough examination in the Foseco laboratory.

The results of this examination are summarised below.

- The entry side of the filters was almost completely covered by a carpet-like coating of material (Figure 5).
- Metallographic examination yielded no evidence of filter reaction or damage.
- The carpet-like coating on one of the filters was subjected to X-ray diffraction analysis (XRD), which confirmed the presence of the following phases: corundum Al<sub>2</sub>O<sub>3</sub>, olivine Mg<sub>2</sub>SiO<sub>4</sub> / (Mg, Fe)<sub>2</sub>SiO<sub>4</sub>, Mg-Al spinel and a Ca-Al oxide (Figure 6).

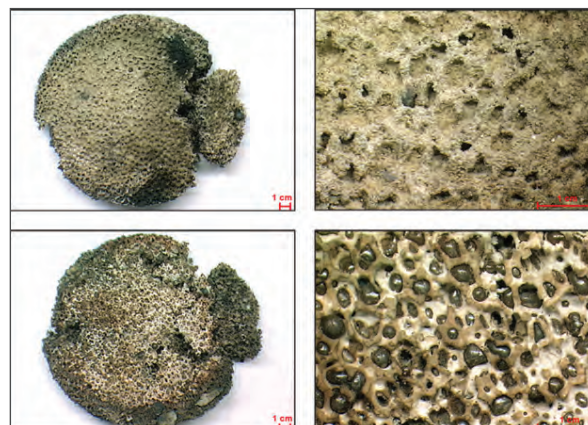


Figure 5. Entry (top) and exit (bottom) sides of an affected filter - the entry side of the filter is covered with an almost unbroken layer of carpet-like material

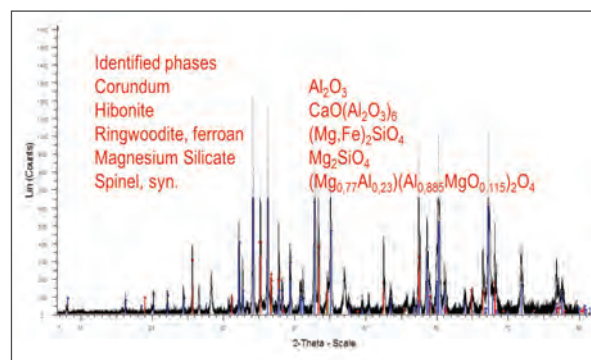


Figure 6. X-ray diffraction analysis of the layer of carpet-like material

The phases corundum Al<sub>2</sub>O<sub>3</sub> and Mg-Al spinel (Figure 6) revealed by the x-ray diffraction suggested that the layer of carpet-like material blocking the filter on the input side consists primarily of residues from the furnace or ladle linings.

On the basis of these results, the furnace operation procedure (that was documented during the tests) was re-examined (Table 1). This examination showed that the furnaces were only 60% filled at the time when the two batches were melted where filter blockages occurred. The furnaces were at least approx. 70% filled for all other batches. This gave grounds for supposing that the higher capacity density in the induction furnaces led to increased melt mobility, resulting in a greater degree of erosion of the refractory linings. Higher furnace temperatures also tend to favour such processes.

Batch	Material	Casting Piece	Furnace content [kg]	T max. (furnace) [°C]	T (tapping) [°C]	T (ladle) [°C]
1	G 35 CrMoV 10 4	A	2060	1655	1655	1623
2	G 35 CrMoV 10 4	A	2060	no data	1665	1616
3	G 42 CrMo 4	B	2450	1665	no data	1607
4	G 42 CrMo 4	B	2505	no data	no data	1610
5	G 42 CrMo 4	B	2200	1686	1645	1603
6	G 42 CrMo 4	B	1915	1664	1634	1608
7	G 42 CrMo 4	B	1835	1642	1638	1607
8	G 30 NiCrMo 14	C	1710	no data	1640	1620
9	G 30 NiCrMo 14	C	2240	no data	1640	1618
10	GS-52.3	D	2115	1650	no data	1605
11	GS-52.3	D	1470	no data	no data	1631
12	GS-52.3	D	1470	1662	no data	1622
Mean value			2002.5	1660.6	1645.3	1614.2
Min.			1470	1642	1634	1603
Max.			2505	1686	1665	1631

Table 1. Overview of test furnace batches (no data: was not determined, red: filter blockages)

As a result, the following measures were agreed in cooperation with the foundry management:

- furnaces to be filled fully (2500 kg) in order to reduce potential for erosion of the refractory linings
- avoid exceeding the tapping temperature (1640 °C)
- careful de-slagging the furnaces using SLAX\* 30

As a next step, four casting were poured from one batch applying the measures detailed above. The test was carried out with a newly lined furnace. The filters used in this test provided values of 0.260-0.279 g/cm<sup>3</sup> and 36.7-38.1 mbar for bulk density and pressure drop respectively. No filter blockages occurred.

After this, the boundary conditions were made increasingly more severe. Additional eight castings were poured from two batches using the alloy GS-52.3. In order to verify if the measures taken gave the desired process reliability, the tests were carried out in a furnace in which 38 batches had been previously melted. The bulk density and pressure drop figures for the filters used here were 0.255-0.282 g/cm<sup>3</sup> and 36.2-43.6 mbar respectively. Despite the fact that the bulk density and pressure loss figures were high in some cases, once again no filter blockages occurred.

In the subsequent course of the tests a further 15 castings were poured from four batches. The casting concerned is normally manufactured using STELEX Pro Ø200x35 10 ppi filters, however to confirm the effectiveness of the measures adopted to prevent filter blockage these castings were produced with STELEX Pro Ø175x35 10 ppi filters. Using a STELEX Pro Ø200x35 10 ppi filter, the specific filter capacity was 1.72 kg/cm<sup>2</sup>. Eight of the 15 castings were poured using a STELEX Pro Ø175x35 10 ppi filter, thus increasing the specific filter capacity to 2.25 kg/cm<sup>2</sup>. Here, too, no filter blockages were observed. The bulk densities and pressure drop values

for the filters used in these tests, as well as the alloy, are given in Figure 7.

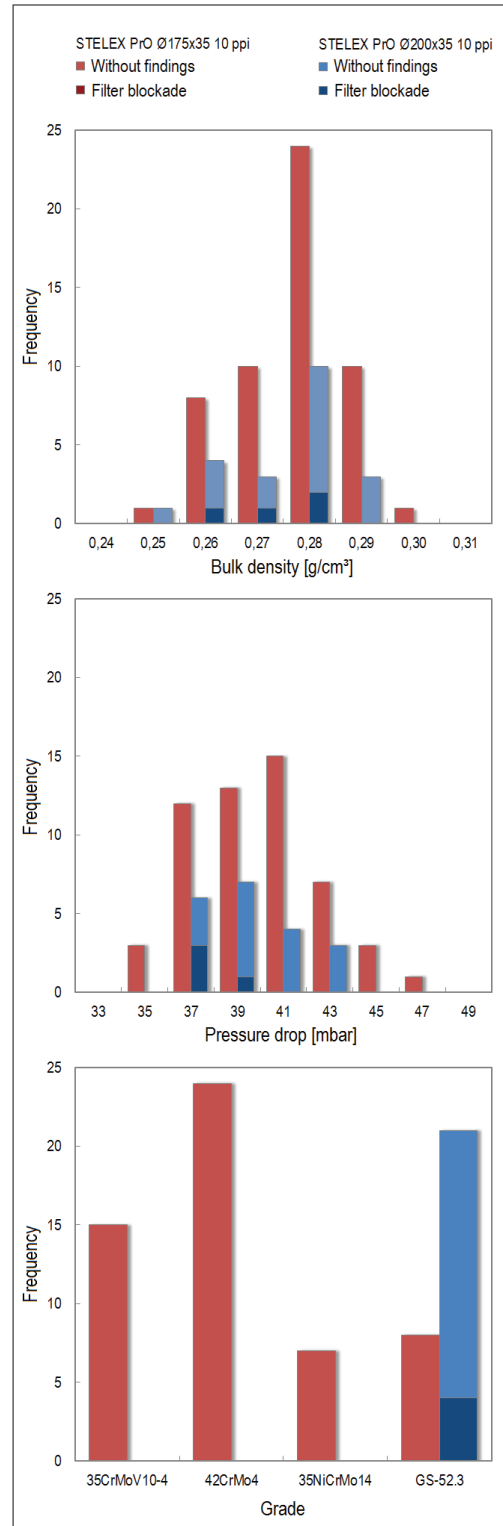


Figure 7. Bulk density (top), pressure drop (centre) of the filters used in the casting tests and the steel grade (bottom)

---

The results of this study were later confirmed on the basis of evaluating the annual consumption of refractory lining and repair materials used in the furnaces. The annual consumption of lining and repair material was found to have increased compared to the previous year by 16% / 55%, whilst the cast tonnage remained much the same.

It is clear that in series production on an industrial scale it is very difficult to maintain and keep a check on the measures that were implemented here by way of immediate corrective action. In view of this, the refractories used in the furnaces were checked for suitability and replaced by better-quality materials.

### Summary

The case study presented here shows that filter blockages do not necessarily arise as a result of the filter characteristics. Of particular significance are the type and quantity of the non-metallic contaminants in the molten metal, that are subsequently removed by the filter and which ultimately can lead to filter blockage. In the case investigated here, the blockages occurred with STELEX PrO filters whose bulk density and pressure drop values were relatively low. This showed that the filters used were themselves not the cause of the filter blockages. The origin of the layer of residue on a blocked filter could be traced to the furnace linings through XRD analysis of the constituent phases. When the agreed measures were adopted, it was possible to manufacture the casting reliably using a smaller STELEX PrO Ø175x35 10 ppi filter.

### References

[1] BDG-Richtlinie P100: Keramische Filter in Schaumstruktur – Schaumkeramikfilter für Eisen und Stahlguss, October 2013. [Federation of the Germany Foundry Industry Directive: Ceramic Foam Filters for Iron and Steel Casting]

[2] Midea, A.: Pressure drop characteristics of iron filters. Foundry Practice 243 (2001).

### Links

Scan this QR code with your smartphone to view a video relating to this paper.



Mode of operation of filter media



# Just **add** Foseco

Responding to the increasing challenges you face, Foseco simplifies your operations, providing innovative solutions that deliver real world results.

For over eight decades we've sustained an unrivalled reputation for game-changing ideas, adding new value to almost everything you do. And, by consistently ensuring premium quality results, we're now the partner of choice for foundries worldwide.

So, release your true potential: **just add Foseco.**

- + Partnership
- + Global Technology - Locally Delivered
- + Creative, Innovative Solutions
- + Expert Advice
- + Reliability
- + Knowledge Leadership

+49 2861 83 207

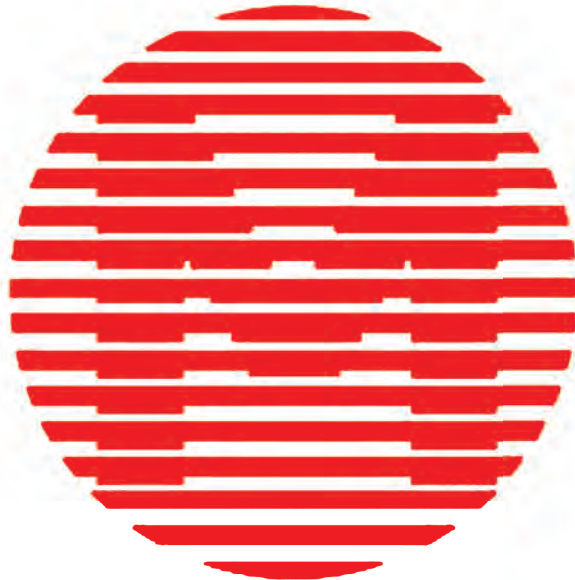
[www.foseco.com](http://www.foseco.com)



# Visit Foseco...



World Foundry Congress  
Bilbao, Spain from 19th - 21st May 2014



China International Foundry Expo  
Beijing, China from 19th - 22nd May 2014

---

All rights reserved. No part of this publication may be reproduced, stored in a retrieval system of any nature or transmitted in any form or by any means, including photocopying and recording, without the written permission of the copyright holder.

All statements, information and data contained herein are published as a guide and although believed to be accurate and reliable (having regard to the manufacturer's practical experience) neither the manufacturer, licensor, seller nor publisher represents or warrants, expressly or impliedly:

- (1) their accuracy/reliability
- (2) that the use of the product(s) will not infringe third party rights
- (3) that no further safety measures are required to meet local legislation

The seller is not authorised to make representations nor contract on behalf of the manufacturer/licensor. All sales by the manufacturer/seller are based on their respective conditions of sale available on request.

\*FOSECO, the logo, ALSPEK, SLAX and STELEX are Trade Marks of the Vesuvius Group, registered in certain countries, used under licence.

© Foseco International Ltd. 2014

#### COMMENT

Editorial policy is to highlight the latest Foseco products and technical developments. However, because of their newness, some developments may not be immediately available in your area. Your local Foseco company or agent will be pleased to advise.

---

**Foseco International Limited**  
P.O. Box 5516  
Tamworth  
Staffordshire  
England B78 3XQ  
Registered in England No. 468147



**ISSN 0266 9994**

Produced in England

**400061135**